Supporting information

Super-flexible phase change materials with a dual-supporting effect for solar thermoelectric conversion in ocean environment

Yi-Cun Zhou, Jie Yang*, Lu Bai, Rui-Ying Bao, Ming-Bo Yang, Wei Yang*

College of Polymer Science and Engineering, Sichuan University, State Key Laboratory of Polymer Materials Engineering, Chengdu 610065, Sichuan, People's Republic of China.

1. Experimental section

1.1. Materials

Phase change microcapsules (PCMCs) with a phase change temperature of 45-50 °C were purchased from Anhui Meikedi Intelligent Microcapsule Technology Co., Ltd. Paraffin wax (PW) with a phase change temperature of 45-50 °C was purchased from Shanghai Jianqiu Chemical Co., Ltd. Natural rubber latex (NRl) with a solid content of 61.5% was obtained from Maoming Zhengmao Petrochemical Co., Ltd. Layered ternary carbide (Ti_3AlC_2) powder was supplied by 11 Technology Co., Ltd. Lithium fluoride (LiF, 98+%) and polypropylene membrane (3501 coated PP) were purchased from Alfa Aesar and Celgard LLC, NC, respectively. Bacterial cellulose (Diameter: 50-100 nm, Length: ~20 μm) aqueous dispersion with a concentration of 0.65 wt% was purchased from Guilin Qihong Technology Co., Ltd. Boron nitride (BN) flakes with an apparent density of 2.25 g/cm^3 and particle size of 5-15 μm were supplied by Qinghuangdao ENO High-Tech Material Development Co., Ltd. Deionized water was made by a standard ultrapure water machine (UPH-IV-5/10/20 T), Sichuan Youpu Ultrapure Technology Co., Ltd. Sodium hydroxide (NaOH), 9 M hydrochloric acid (HCl), sodium chloride (NaCl), and ethanol were supplied by Haihong Chemical Reagents Company (Chengdu, China). All solvents and reagents were directly used as received without further purification.

1.2 Synthesis of 2D MXene nanosheets

MXene ($Ti_3C_2T_x$) nanosheets were synthesized by etching the Al phase of Ti_3AlC_2 with LiF/HCl solution. Typically, 1 g LiF was dissolved in 20 mL 9M HCl in a Teflon container under magnetic stirring for 10 min. Then, 1 g Ti_3AlC_2 powder was slowly

Corresponding author. Tel.: + 86 28 8546 0130; fax: + 86 28 8546 0130.

E-mail address: psejieyang@scu.edu.cn (J Yang), weiyang@scu.edu.cn (W Yang)

added into the LiF/HCl etching solution, and the mixture reacted at 40 °C for 36 h under magnetic stirring to obtain the $Ti_3C_2T_x$ suspension. The resulting $Ti_3C_2T_x$ suspension was repeatedly washed with deionized water and centrifuged at 4000 rpm for 5 min until pH > 5. The obtained $Ti_3C_2T_x$ solution was frozen at -20 °C for 12 h. The delamination of $Ti_3C_2T_x$ was performed by sonication treatment, followed by the centrifugation for 2 h at 3500 rpm to obtain a homogeneous supernatant with delaminated 2D MXene nanosheets. The concentration of the resultant MXene solution was identified by filtering the solution of a known volume with a polypropylene membrane (Celgard 3501 coated PP) and measuring the weight of the resulting freestanding film after vacuum drying. The P-type and N-type legs in the thermoelectric unit are antimony-doped bismuth telluride and selenium-doped bismuth telluride, respectively.

1.3 Fabrication of super-flexible phase change materials (SFPCMs)

According to the PCMCs loading, the SFPCMs without MXene were denoted as NM50, NM60, and NM70. NM60 was taken as an example, in which the mass fraction of PCMCs in SFPCMs was 60%. First, 13 g NRl was diluted with 15 mL deionized water, followed by mixing with 12 g PCMCs and mechanically stirring for 10-15 min. The hybrid slurry was poured into a mold and then placed in an oven at 120 °C for 2 h after drying at 40 °C for 24 h. NM50 and NM70 were prepared in a similar manner. For SFPCMs with MXene, 5 mL, 10 mL and 15 mL MXene aqueous dispersions with a concentration of 8 mg/mL were added to diluted NRl solutions, followed by magnetically stirring for 15 min. After that PCMCs were added and stirred for 20 min. The as-prepared mixtures were poured into molds and dried at 40 °C for 24 h. Finally, the samples were transferred to an oven at 120 °C for another 2 h, and named as NM60M1, NM60M2 and NM60M3 according to the MXene loading. The final solar thermoelectric device is made by firmly fixing the SFPCMs to the thermoelectric unit with a silicone rubber-based glue.

1.4 Fabrication of 3D skeleton-supporting composite PCMs

The commercial melamine foam (MF) was cut into 20 mm × 20 mm × 10 mm cubes. The PW blocks were placed in a petri dish and transferred to a 90 °C vacuum oven for melting. The MF scaffolds were immersed in molten PW for 48 h to completely remove air bubbles. The resulting MF-supporting PCMs were taken out of the vacuum oven and cured at room temperature, named as MFPCMs. Moreover, 100 g cellulose aqueous

solution with a mass fraction of 0.65% was mixed with 20 g BN powder. The mixture was mechanically stirred and sonicated in an ultrasonic water bath for 20 min. The obtained BN slurry was poured into a cubic mold with a cross section of 20 mm × 20 mm, and then frozen at -18 °C for 24 h. After that the frozen samples were freeze-dried in a vacuum freeze dryer to obtain 3D porous BN scaffolds. Their porosity was maintained above 80% to ensure the filling of PW. Similarly, the aforementioned impregnation process was repeated to prepare the BN/cellulose scaffold-supporting PCMs, named as SPCMs. Finally, the residual PW on the surface of MFPCMs and SPCMs was removed using sandpapers.

2. Characterization

The field-emission scanning electron microscopy (SEM, FEI, Oregon, USA) was employed to observe the morphology of SFPCMs at an accelerating voltage of 5 kV. The size of 2D MXene nanosheets was characterized by atomic force microscope (AFM, Multimode 8, Bruker Corporation) in tapping mode. The morphology of PCMCs before and after phase transition was observed by optical microscopy (Olympus Co., Tokyo, Japan) equipped with a hot stage (LINKAM THMS 600). The particle size distribution of PCMCs was measured by Dry Laser Particle Size Analyzer (HELOS KR, Germany). Fourier transform infrared (FT-IR) spectra of SFPCMs were recorded from 4000 cm^{-1} to 400 cm^{-1} using a Nicolet 6700 FT-IR spectrometer (Thermo Fisher Scientific Inc., Waltham, MA, USA) with a resolution of 4 cm^{-1} in all total reflection (ATR) mode. X-ray diffraction (XRD) analysis was carried out on an X-ray diffractometer (UItima IV, Rigaku, Japan) with Cu Kα radiation (λ = 0.154 nm) from 0° to 80°. To better understand the network structure formed in SFPCMs, the dynamic behaviors of NM60 and NM60M3 at 25 °C and 80 °C were investigated using a rheometer (TA Instruments, AR 2000ex) with a shear strain of 0.01%, and the storage modulus (G') and loss modulus (G'') of the samples were obtained over the shear frequency range of 0.1-100 rad/s. The mechanical properties were characterized using an Instron 5967 universal material testing machine with an extension rate of 20 mm/min according to ASTM D638-10, and each sample was measured five times to calculate the average value. The hardness of the SFPCMs was tested using Shore hardness tester (LX-A, China). A differential scanning calorimetry (DSC, Q20, TA Instruments, USA) was used to investigate thermophysical behaviors. Thermal stability of SFPCMs was

characterized under a nitrogen atmosphere in the temperature range from 30 °C to 800 °C with a heating rate of 10 °C/min using thermogravimetric analysis (TGA, Mettler Toledo TGA-2 system, Mettler Toledo Corp., Switzerland). The light absorption performance was evaluated over a wavelength range of 150 to 2500 nm using an ultraviolet-visible near-infrared (UV-vis-NIR) spectrophotometer (UV3600, Shimadzu, Japan) equipped with an integrating sphere. The thermal conductivity of SFPCMs was measured using a laser flash technique (Netzsch, LFA 467, USA). An infrared thermal imager (Fluke Ti27) was used to intuitively record the temperature distribution of SFPCMs. The simulated sunlight was emitted by a xenon lamp (CEAULIGHT, China), and the optical power density of the light source was checked by an optical power meter (CEAULIGHT, China). The temperature change of samples under illumination was recorded using a paperless recorder with thermocouples (OMEGA). A Keithley 2400S electrometer connecting a computer was used to record output voltage in real time. The photothermal conversion efficiency (η) was calculated by Equation 1:

$$\eta = m\Delta H/\rho S(t_1 - t_0) \quad (1)$$

where m is the total mass of the tested specimen, ΔH is the melting enthalpy of the corresponding specimen measured by DSC, ρ is the irradiation intensity of the simulated light source (150 mW/cm^2 @ AM1.5), S is the surface area of the specimen, and t_0 and t_1 are the time before and after the phase transition of the specimen, respectively.

3. Figures and Tables

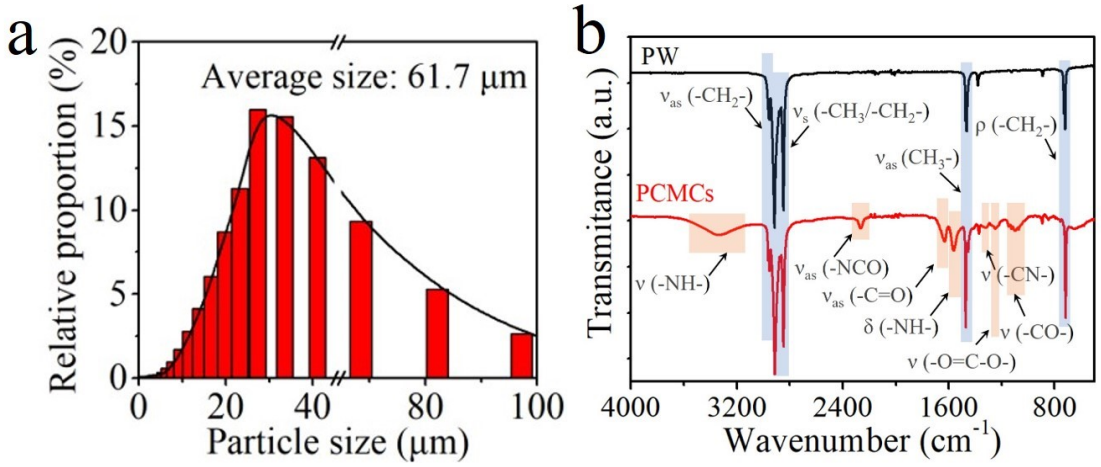

Fig. S1. (a) Size distribution statistics of PCMCs. **(b)** FT-IR spectra of PW and PCMCs.

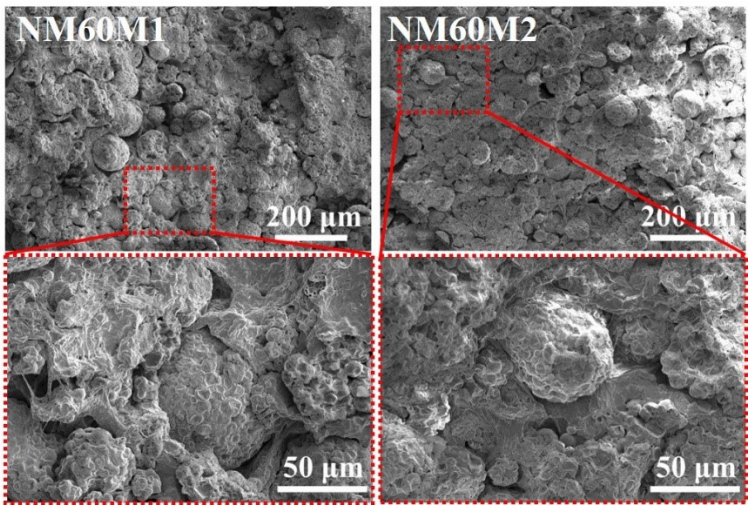

Fig. S2. Cross-sectional SEM images of NM60M1 and NM60M2.

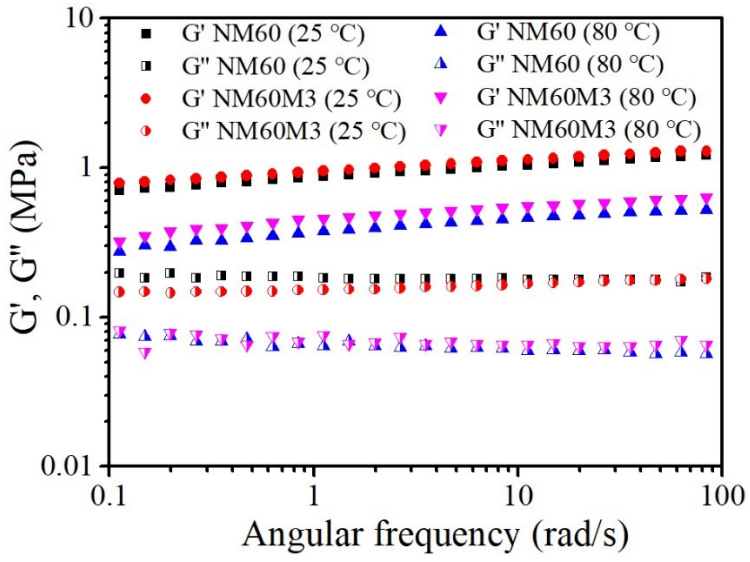

Fig. S3. Rheological behavior of NM60 and NM60M3 at 25 °C and 80 °C.

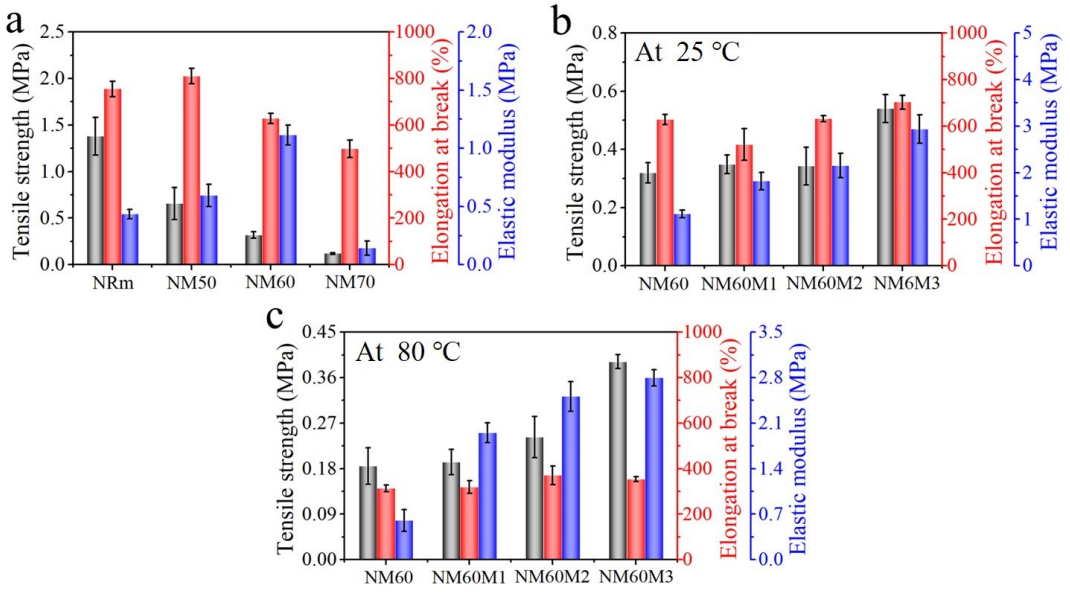

Fig. S4. (a) Statistical mechanical properties of NRm, NM50, NM60, and NM70 at 25 ° C. Statistical mechanical properties of NM60, NM60M1, NM60M2, and NM60M3 at **(b)** 25 °C and **(c)** 80 °C.

Table S1 DSC heating and cooling characteristic parameters of PCMCs and SFPCMs.

Samples	T_c (°C)	ΔH_c (J/g)	T_m (°C)	ΔH_m (J/g)
PCMCs	32.5	207.8	48.1	208.1
NM50	33.3	102.8	47.8	102.7
NM60	33.5	125.8	46.8	126.2
NM70	32.1	143.8	48.2	143.4
NM60M1	32.8	125.7	47.1	126.0
NM60M2	31.8	126.0	47.0	126.4
NM60M3	31.9	126.3	47.4	126.8

Table S2 DSC heating and cooling characteristic parameters of NM60 and NM60M3 before and after 200 melting and crystallization cycles.

Cycles	T_c (°C)	ΔH_c (J/g)	T_m (°C)	ΔH_m (J/g)
NM60 1st	32.7	126.2	47.3	126.8
NM60 51th	32.8	126.8	47.2	127.0
NM60 101th	32.7	126.8	47.3	127.0
NM60 201th	32.5	126.3	47.1	126.6
NM60M3 1st	33.5	126.8	47.4	127.1
NM60M3 51th	32.6	126.7	47.3	127.2
NM60M3 101th	32.6	126.8	47.2	127.1
NM60M3 201th	32.5	126.3	46.8	126.8

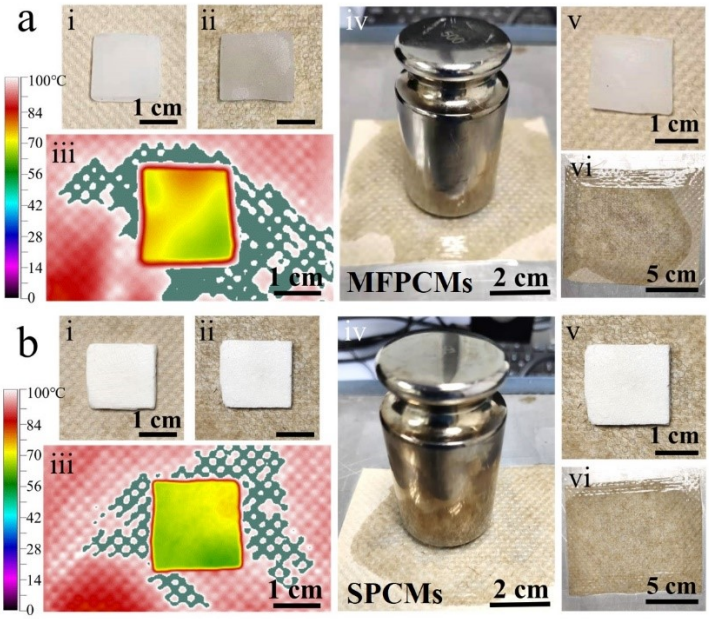

Fig. S5. Anti-leakage properties of melamine foams based PCM (MFPCM, **a**) and BN/cellulose scaffold-supporting PCMs (SPCMs, **b**). and digital images of samples (i), digital images of sample after phase transition (ii), IR images of samples after phase transition (iii), digital images

of samples after phase transition at 500 g weight (iv), images of samples without weight (v), and images of oil-absorbing paper after sample removal (vi).

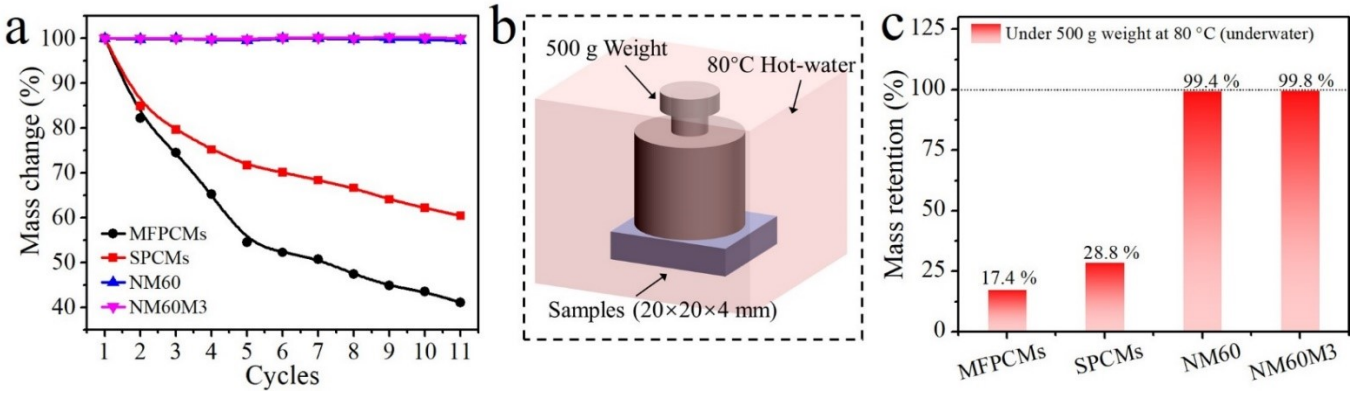

Fig. S6. (a) Mass evolution curves of MFPCMs, SPCMs, NM60, and NM60M3 after 10 melting/crystallization cycles in an 80 °C oven. **(b)** Experimental design of shape stability test under force when the samples are underwater phase change state. **(c)** Mass retention of MFPCMs, SPCMs, NM60, and NM60M3 after compressed by a 500 g load under 80 °C water.

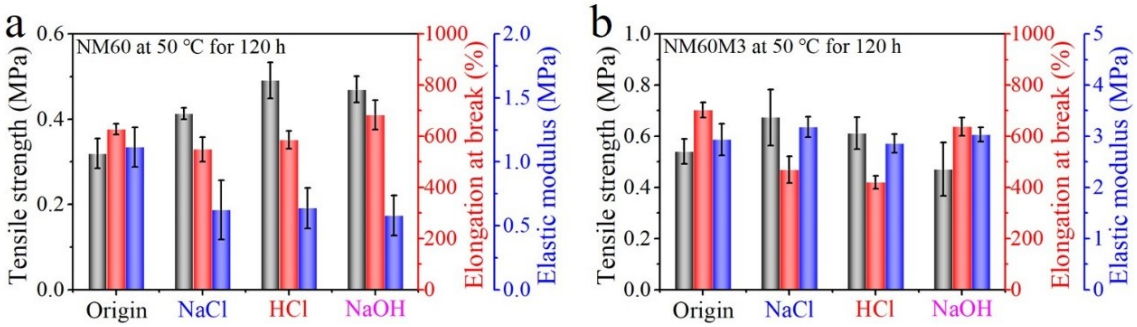

Fig. S7. Statistical mechanical properties of **(a)** NM60 and **(b)** NM60M3 after the treatment in saturated NaCl solution, 2 M HCl solution, and 2 M NaOH solution for 120 h at 50 °C.

Table S3 DSC heating and cooling characteristic parameters of NM60 and NM60M3 after the treatment in saturated NaCl solution, 2 M HCl solution, and 2 M NaOH solution for 120 h at 50 °C.

Samples	T_c (°C)	ΔH_c (J/g)	T_m (°C)	ΔH_m (J/g)
NM60	33.5	125.8	46.8	126.2
NM60 (NaCl)	32.3	124.3	45.4	124.6
NM60 (HCl)	31.4	124.6	47.1	125.3
NM60 (NaOH)	31.6	124.4	47.5	124.7
NM60M3	32.0	126.3	47.4	126.8
NM60M3 (NaCl)	31.8	126.5	46.6	126.6
NM60M3 (HCl)	31.6	126.4	46.6	126.8
NM60M3 (NaOH)	31.8	126.1	47.8	126.8

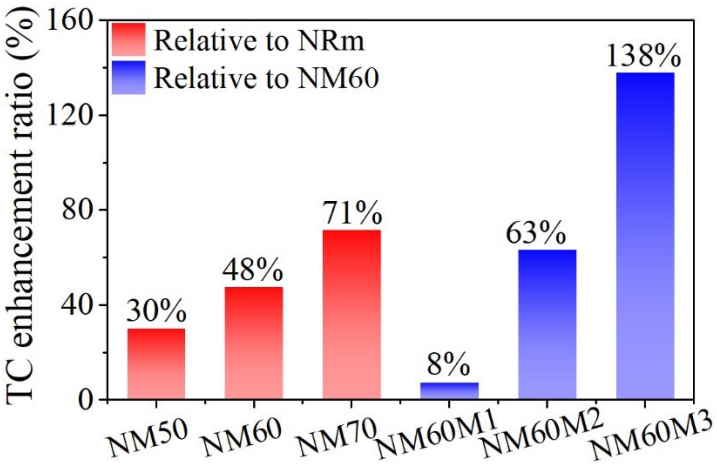

Fig. S8. Thermal conductivity (TC) changes of NM50, NM60 and NM70 with respect to NRm (0.11 W/m K), and thermal conductivity changes of NM60M1, NM60M2 and NM60M3 with respect to NM60 (0.16 W/m K).

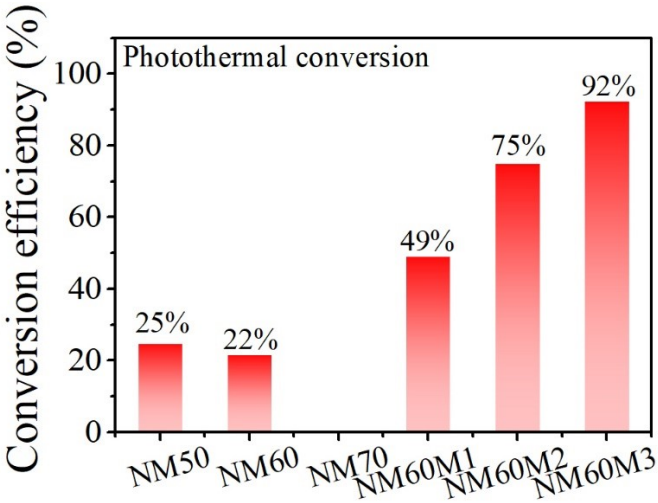

Fig. S9. Photothermal conversion efficiencies of SFPCMs. Given no phase transition occurs for NM70, we cannot obtain its photothermal conversion efficiency.

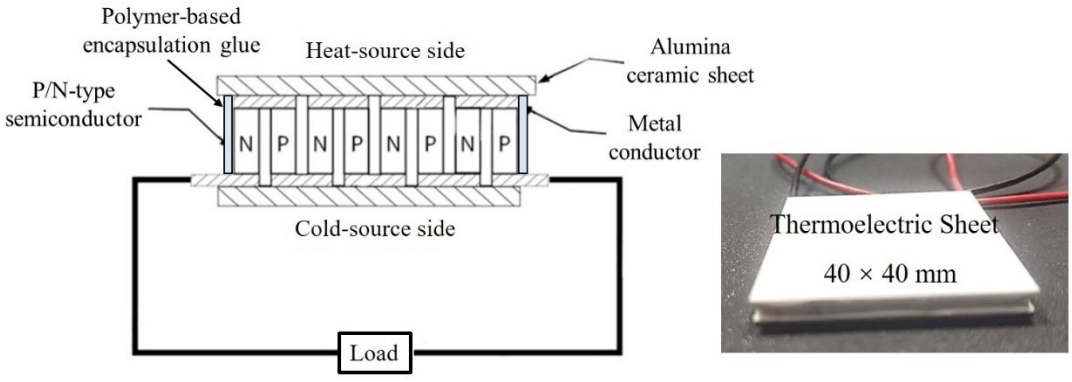

Fig. S10. Structure of the thermoelectric unit in STEGs.

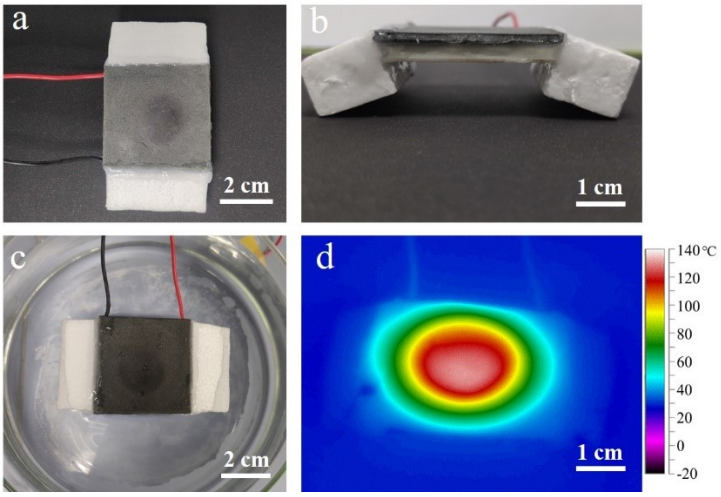

Fig. S11. A self-floating photoelectric conversion device (NM60M3-D) based on NM60M3 and thermoelectric modules. **(a)** Top view and **(b)** front view of NM60M3-D. **(c)** Top view of NM60M3-D floating on the water surface. **(d)** Infrared thermal image of NM60M3-D under the irradiation with an intensity of 200 mW/cm^2.